

**Manipulating valence and core electronic excitations of a transition metal
complex using UV/Vis and X-ray cavities**

Bing Gu,¹ Stefano M. Cavaletto,¹ Daniel R. Nascimento,²
Munira Khalil,³ Niranjan Govind,² and Shaul Mukamel^{1,*}

¹*Department of Chemistry and Department of Physics & Astronomy,
University of California, Irvine, CA 92697, USA*

²*Physical and Computational Sciences Directorate,*

Pacific Northwest National Laboratory, Richland, WA 99352, USA

³*Department of Chemistry, University of Washington, Seattle, Washington 98115, USA*

* smukamel@uci.edu

CONTENTS

S1. Computational details of valence- and core-polariton states	S2
S1.A. Transition dipole moments between polariton states	S3
S2. Absorption Spectrum for a system with a non-Hermitian Hamiltonian	S3
S3. SXRS Simulations	S4
References	S4

S1. COMPUTATIONAL DETAILS OF VALENCE- AND CORE-POLARITON STATES

For the UV/Vis cavity, the valence-polaritons and cavity-modified core-excitations are computed by diagonalizing the polaritonic Hamiltonian in the direct product basis $\{ |gn\rangle, |v_\alpha n\rangle \}$, $n = 0, 1, \dots$. The maximum cavity photon number state considered in the computations is 5. The valence polaritons are computed using a Hermitian Hamiltonian as the decay rates of valence excitations and the cavity mode are small. The valence-polariton lifetime, arising from both the exciton decay and cavity decay, is accounted for phenomenologically by setting $\tilde{\omega}_\mu = \omega_\mu - i\gamma_\mu$ where $\gamma_\mu = 0.05$ eV. The influence of an UV/Vis cavity mode to the electronic structure of molecules is two fold. In the UV/Vis regime, the cavity mode hybridizes with the valence excitation leading to valence polaritons. The second effect is on the valence excitations in the presence of a core-hole (core-excited valence excitations).

The UV/Vis and X-ray cavity-modified core-excitations are obtained with a non-Hermitian Hamiltonian. The core-exciton decay rate is computed with Eq. (3) in the main text. For an UV/Vis cavity mode with quality factor $Q > 100$, its decay rate is much smaller than the decay rates of core-excited states ($2 \sim 8$ eV). Thus, the cavity decay does not affect the results and was set to 0 for computations involving core-excitations. The X-ray cavity decay is assumed to be $\kappa = 0.5$ eV.

The relative strength of electric dipole and electric quadrupole coupling is given by

$$\eta_{\beta\alpha} = \frac{-\boldsymbol{\mu}_{\beta\alpha} \cdot \mathbf{E}(\mathbf{r}_0)}{-\frac{1}{2}\mathbf{Q}_{\beta\alpha} : \boldsymbol{\nabla} \otimes \mathbf{E}(\mathbf{r}_0)} \quad (\text{S1})$$

where $\mathbf{A} : \mathbf{B} = \sum_{i,j} A_{ij}B_{ij}$ denotes tensor contraction. For ferricyanide, the electric quadrupole coupling is much smaller ($\eta \sim 1/100$) than the electric dipole coupling, and is thus not included in the computations of polaritons and signals. Nevertheless, it is possible to place the materials

in the nodes of the cavity mode function where the leading cavity-molecule coupling will be the electric quadrupole.

S1.A. Transition dipole moments between polariton states

The transition dipole moment (TDM) matrix elements between different states are required for computing the signals. The TDM between valence-polaritons $|e_\beta\rangle$ and cavity-modified core-excited states $|f_\nu\rangle$ are constructed as

$$\begin{aligned}\langle e_\beta|\boldsymbol{\mu} \otimes \mathbf{I}_c|f_\nu\rangle &= \sum_{\alpha,\mu} \sum_{n,m=0,1,\dots} \langle e_\beta|v_\alpha n\rangle \langle v_\alpha n|\mu|c_\mu m\rangle \langle c_\mu m|f_\nu\rangle \\ &= \sum_{\alpha,\mu} \sum_{n=0,1,\dots} \langle e_\beta|v_\alpha n\rangle \langle v_\alpha|\mu|c_\mu\rangle \langle c_\mu n|f_\nu\rangle\end{aligned}\quad (\text{S2})$$

where \mathbf{I}_c is the identity operator of the cavity and $\boldsymbol{\mu} = \boldsymbol{\mu} \cdot \mathbf{e}_c$ is the electric dipole operator projected on the cavity-mode polarization. In Eq. (S2), we have used that fact that the polariton states are a linear combination of $|gn\rangle \equiv |g\rangle \otimes |n\rangle_c$ and $|v_\alpha m\rangle$. Note that in Eq. (S2) the ground state has to be included in the set $|v_\alpha\rangle$. Similarly, the TDM between $|f\rangle$ and the ground state is given by

$$\langle f_\nu|\boldsymbol{\mu} \otimes \mathbf{I}_c|g0\rangle = \sum_{\beta} \langle f_\nu|c_\beta 0\rangle \langle c_\beta|\boldsymbol{\mu}|g\rangle \quad (\text{S3})$$

where $|c_\beta\rangle$ runs over the 200 core-excited states from the electronic structure computations.

Since the $|f\rangle$ states are obtained by diagonalizing a non-Hermitian matrix \tilde{H} , for each $|f_\nu\rangle$, there is a corresponding state $|\tilde{f}_\nu\rangle$ satisfying that $\tilde{H}^\dagger|\tilde{f}_\nu\rangle = \tilde{\omega}_\nu^*|\tilde{f}_\nu\rangle$. The TDM matrix elements $\langle e_\beta|\boldsymbol{\mu}|\tilde{f}_\nu\rangle$ are also required for the spectroscopic computations and can be computed similarly as in Eq. (S2).

S2. ABSORPTION SPECTRUM FOR A SYSTEM WITH A NON-HERMITIAN HAMILTONIAN

The absorption signal employs a single pulse and measures the attenuation of the pulse after transmitting through the sample. The signal is given by

$$A(\omega) = 2 \operatorname{Re} \int_0^\infty dt e^{i\omega t} \langle V(t)V^\dagger \rangle. \quad (\text{S4})$$

where V (V^\dagger) is the lowering (raising) component of the dipole operator, $-\boldsymbol{\mu} = V + V^\dagger$. Introducing $|f_\nu\rangle$ the right eigenvector of the non-Hermitian polaritonic Hamiltonian

$$\tilde{H}|f_\nu\rangle = \tilde{\omega}_\nu|f_\nu\rangle \quad (\text{S5})$$

and $|\tilde{f}_\nu\rangle$ the right eigenvector of \tilde{H}^\dagger , $\tilde{H}^\dagger |\tilde{f}_\nu\rangle = \tilde{\kappa}_\nu |\tilde{f}_\nu\rangle$, the two sets of states satisfy

$$\langle \tilde{f}_\nu | f_{\nu'} \rangle = \delta_{\nu\nu'} \langle \tilde{f}_\nu | f_\nu \rangle. \quad (\text{S6})$$

We assume that for each $\tilde{\omega}_\nu$ there is a $\tilde{\kappa}_\nu = \tilde{\omega}_\nu^*$ such that there is a correspondence between $|f_\nu\rangle$ and $|\tilde{f}_\nu\rangle$. In terms of the bi-orthogonal basis set, the propagator for a non-Hermitian system can be written as

$$\tilde{U}(t) = \sum_\nu e^{-i\tilde{\omega}_\nu t} \frac{|f_\nu\rangle \langle \tilde{f}_\nu|}{\langle \tilde{f}_\nu | f_\nu \rangle} \quad (\text{S7})$$

Inserting Eq. (S7) into Eq. (S4) leads to

$$A(\omega) = \sum_\nu -2 \text{Im} \frac{\langle g | \mu | f_\nu \rangle \langle \tilde{f}_\nu | \mu | g \rangle}{(\omega - \tilde{\omega}_\nu) \langle \tilde{f}_\nu | f_\nu \rangle} \quad (\text{S8})$$

For Hermitian systems, $|\tilde{f}_\nu\rangle = |f_\nu\rangle$, and Eq. (S8) reduces to the conventional linear absorption expression for Hermitian systems.

S3. SXRS SIMULATIONS

The complex frequencies $\tilde{\omega}_\nu$ of the hybridized core states are obtained by diagonalizing the non-Hermitian Hamiltonian of Eq. (S5), while the complex frequencies of the valence-polaritons $\tilde{\omega}_\beta = \omega_\beta - i\gamma_\beta$ account for a constant width $\gamma_\beta = 0.05 \text{ eV}$. In order to excite a large manifold of core and valence states, broadband coherent Gaussian pulses are assumed,

$$E(\omega) = \int E(t) e^{i\omega t} dt = E_0 e^{-\frac{(\omega - \omega_X)^2}{2\sigma^2}}, \quad (\text{S9})$$

with central frequency $\omega_X = 7132 \text{ eV}$ and bandwidth $\sigma = 24 \text{ eV}$, corresponding to a 40 as (intensity FWHM) duration.

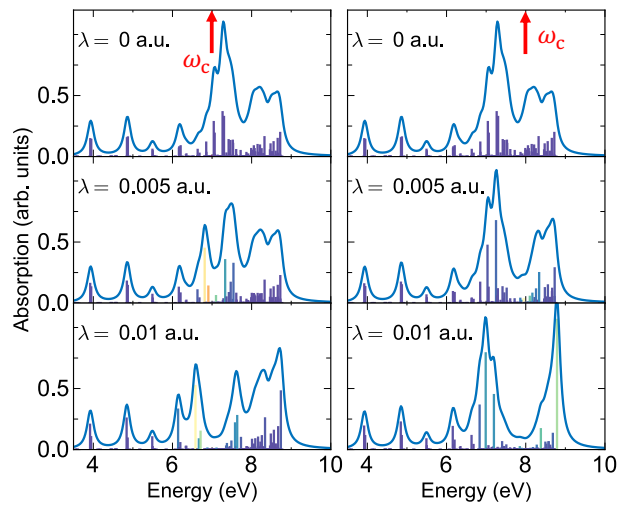


FIG. S1. Same as Fig. 2 but excluding the high-lying valence-excited states with $\omega > 9$ eV.